

# Colorimetric and Electrochemical Bacteria Detection Using Printed Paper- and Transparency-Based Analytic Devices

Jaclyn A. Adkins,<sup>†</sup> Katherine Boehle,<sup>†</sup> Colin Friend,<sup>‡</sup> Briana Chamberlain,<sup>§</sup> Bledar Bisha,<sup>||</sup> and Charles S. Henry<sup>\*,†,‡,§,ID</sup>

<sup>†</sup>Department of Chemistry, <sup>‡</sup>School of Biomedical Engineering, and <sup>§</sup>Chemical and Biological Engineering, Colorado State University, Fort Collins, Colorado 80523, United States

<sup>||</sup>Department of Animal Science, University of Wyoming, Laramie, Wyoming 82071, United States

## Supporting Information

**ABSTRACT:** The development of transparency-based electrochemical and paper-based colorimetric analytic detection platforms is presented as complementary methods for food and waterborne bacteria detection from a single assay. *Escherichia coli* and *Enterococcus* species, both indicators of fecal contamination, were detected using substrates specific to enzymes produced by each species.  $\beta$ -galactosidase ( $\beta$ -gal) and  $\beta$ -glucuronidase ( $\beta$ -glucur) are both produced by *E. coli*, while  $\beta$ -glucosidase ( $\beta$ -gluco) is produced by *Enterococcus* spp. Substrates used produced either *p*-nitrophenol (PNP), *o*-nitrophenol (ONP), or *p*-aminophenol (PAP) as products. Electrochemical detection using stencil-printed carbon electrodes (SPCEs) was found to provide optimal performance on inexpensive and disposable transparency film platforms. Using SPCEs, detection limits for electrochemically active substrates, PNP, ONP, and PAP were determined to be 1.1, 2.8, and 0.5  $\mu$ M, respectively. A colorimetric paper-based well plate system was developed from a simple cardboard box and smart phone for the detection of PNP and ONP. Colorimetric detection limits were determined to be 81  $\mu$ M and 119  $\mu$ M for ONP and PNP respectively. While colorimetric detection methods gave higher detection limits than electrochemical detection, both methods provided similar times to positive bacteria detection. Low concentrations ( $10^1$  CFU/mL) of pathogenic and nonpathogenic *E. coli* isolates and ( $10^0$  CFU/mL) *E. faecalis* and *E. faecium* strains were detected within 4 and 8 h of pre-enrichment. Alfalfa sprout and lagoon water samples served as model food and water samples, and while water samples did not test positive, sprout samples did test positive within 4 h of pre-enrichment. Positive detection of inoculated ( $2.3 \times 10^2$  and  $3.1 \times 10^1$  CFU/mL or g of *E. coli* and *E. faecium*, respectively) sprout and water samples tested positive within 4 and 12 h of pre-enrichment, respectively.



Of all contaminants found in food and water (bacterial, viral, chemical, etc.), bacterial contamination causes the highest number of hospitalizations and deaths within the United States annually.<sup>1,2</sup> Whereas drinking polluted water can lead to illness, the use of unsafe water for irrigation can also contaminate agricultural products causing foodborne illness.<sup>3,4</sup> Leafy greens, for example, are responsible for 46% of foodborne outbreaks within the United States and, because alfalfa sprouts are cultivated in a moist humid growth environment that facilitates bacterial growth, they are one of the leading sources of multistate foodborne outbreaks.<sup>5,6</sup> Human and animal excreta (primarily feces) are major sources of food and waterborne diseases, but it is impossible to test for all possible transferable pathogens in a comprehensive manner.<sup>7</sup> Instead, general indicators for bacterial contamination are commonly detected, and both *E. coli* and *Enterococcus* spp. are used as standard fecal indicator bacteria (FIB).<sup>8–11</sup> *E. coli* and enterococci are found in high concentrations,  $10^9$  and  $>10^4$  colony forming units (CFU) per wet gram of stool, respectively, predominantly in the gut of warm-blooded

animals. Their presence is an indication of not only fecal contamination but also if conditions are amenable for the presence of other pathogens.<sup>11,12</sup> FDA guidance and compliance regulations for both the agricultural production and industrial processing of food and beverages now call for the frequent testing of FIB species, necessitating the need for more portable, inexpensive, and simple to use methods of testing.<sup>13</sup>

Because of the harmful role bacterial infection can play in human health, numerous bacteria detection methods have been developed. Common methods for bacterial detection include immunoassays, DNA amplification/detection methods such as polymerase chain reaction (PCR) and traditional culture methods.<sup>14,15</sup> While DNA and immunoassays have advantages such as selectivity and sensitivity, both can suffer from inhibition effects from sample components that lead to false positives or negatives as well as high instrumentation and/or

**Received:** December 17, 2016

**Accepted:** February 22, 2017

**Published:** February 22, 2017

test costs.<sup>16,17</sup> As a result, the gold standard for bacterial detection has remained culture-based methods.<sup>18</sup> Culturing microorganisms allows for sensitive isolation and confirmation of live target bacteria. Nonselective and selective media are used sequentially in conjunction with biochemical testing and microscopy, making this method time and material intensive. The need for improved bacteria detection methods has led to the development of sensors and analytical methods, including the use of paper-based analytical devices (PADs). PADs provide a simple, easily modifiable, and mass produced alternative platform and can be incorporated with several different detection motifs.<sup>19,20</sup>

Recently, we published paper-based methods for detecting *Salmonella spp.*, *Listeria monocytogenes*, and *E. coli* from food and water samples.<sup>21,22</sup> Briefly, chromogenic reagents were stored in paper-based devices and, after a pre-enrichment culturing step using portable sampling and culture methods (MMS and "Phast Swab"), the sample was added to the device for selective detection of enzymes produced by each bacterial species tested. Compared to conventional culture-based detection, the method reduced reagent consumption and waste generation used an easily disposable and inexpensive substrate (paper) for both reaction and detection, while providing semiquantitative measurements of bacteria concentration. Only a few further examples of paper-based bacteria detection have been presented in the literature.<sup>23–27</sup> The majority of these reports use colorimetric detection with only one example of paper-based electrochemical detection for immunoassay impedance measurements.<sup>28</sup>

While paper-based colorimetric detection can provide a simple visual analysis method, electrochemical detection is not limited by background sample coloration and can potentially provide lower detection limits and easily quantifiable and portable results using existing hand-held and cellphone-based potentiostats.<sup>28–32</sup> Electrochemistry has been previously reported for detection of bacterial enzymes. The majority of assays detected  $\beta$ -gal activity via the production of electrochemically active PAP from *p*-aminophenyl galactopyranoside (PAP-gal) substrate.<sup>33–38</sup> The use of substrates that produce chlorophenol red,<sup>39</sup> naphthoquinones, and resorufin have also been described for electrochemical *E. coli* detection.<sup>40</sup> Electrode modification using enzymes or immobilized live bacteria have been employed to convert  $\beta$ -gal produced phenol<sup>41,42</sup> or PNP,<sup>43</sup> respectively, to more easily detected products. Both modification methods, however, result in sensors undergoing a more complicated reaction process.

Herein, we report improvements in our bacterial detection system, including comparison of colorimetric and electrochemical detection methods. Our colorimetric system uses a smart phone to monitor the reaction as a function of time in paper-based wells as opposed to end point measurements.<sup>44</sup> A platform for electrochemical detection was also developed, and it was determined that transparency film substrates provided the best performance. We determined optimal colorimetric and electrochemical enzymatic assay conditions for detection of the FIB bacteria, *E. coli* and *Enterococcus spp.*, via their production of species indicative enzymes. Both  $\beta$ -galactosidase and  $\beta$ -glucuronidase were used for *E. coli* detection and  $\beta$ -glucosidase for *Enterococcus spp.* detection. Because of their association with coliforms and FIB, these enzymatic reactions are also used as indicators of microbial safety.<sup>45</sup> Substrates for each enzyme produced either ONP or PNP, enabling dual colorimetric and electrochemical detection of bacteria. To our knowledge, this is

the first time either of these substrates have been directly oxidized for the electrochemical detection of bacteria specific enzyme metabolism. Figure 1 shows the overall reaction

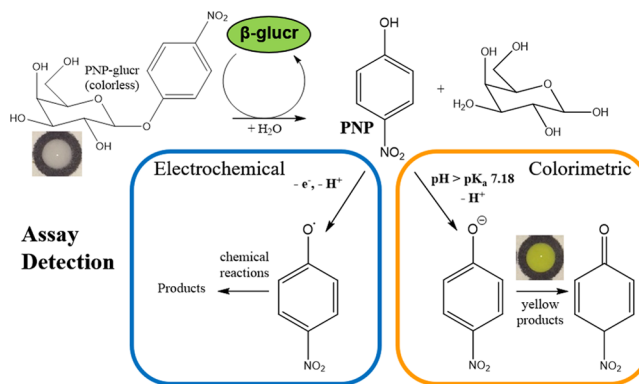


**Figure 1.** Reaction scheme showing the dual electrochemical and colorimetric detection of formed PNP from reacting bacterially produced  $\beta$ -glucr with PNP-glucr.

scheme for reacting a substrate with enzyme and detecting a formed product both electrochemically and colorimetrically. Additionally, this also represents the first example of electrochemical detection of *Enterococcus spp.* using bacterial enzymes as analytes. Pathogenic and nonpathogenic strains of *E. coli* as well as *Enterococcus faecalis* and *E. faecium* were detected in pure culture as well as model surface irrigation water (uninoculated and inoculated lagoon water) and model food samples (uninoculated and inoculated alfalfa sprouts).

## MATERIALS AND METHODS

**Materials and Reagents.** A full list of materials and reagents used can be found in the *Supporting Information*.

**Device Fabrication.** The fabrication processes for making paper-based well devices<sup>21</sup> and electrochemical paper-based<sup>46</sup> and transparency film-based devices<sup>47</sup> have been previously described. A brief description can be found in the *Supporting Information*. Paper-based well plates consisted of 7 columns and 12 rows for a total of 84 wells that were each 6 mm in diameter (inner) after melting and held 50  $\mu$ L of total solution volume when wetted.

Electrodes were printed onto transparency film, Whatman, or copy paper and the device designs and printing process are shown in Figure S1 and Figure 2. Similar to paper-based devices, the entire printed sheet is flexible and contains 240 devices (Figure 2A,B) with electrode geometries shown in Figure 2C. A small layer of silver paint was applied to the reference electrode within the well to serve as a Ag/AgCl reference with the presence of 0.4 M Cl<sup>-</sup> in tested solutions (Figure 2C). Each electrode can hold 30  $\mu$ L of solution (Figure 2D).

**Colorimetric Assay Detection.** For quantitation of colorimetric products, a "light box" and the camera of an iPhone 5S were used to capture images (Figure 3A). The light box was fabricated by lining a cardboard box (16 cm  $\times$  16 cm  $\times$  16 cm) with white copy paper and cutting a small opening (2 cm  $\times$  5 cm) at the top to accommodate the camera phone. For each experiment, three samples of each reaction (replicate measurements) were placed in every other column (Figure 3B). The columns on each side of the samples contained DI water, which acted as lighting controls. Because of the inconsistent

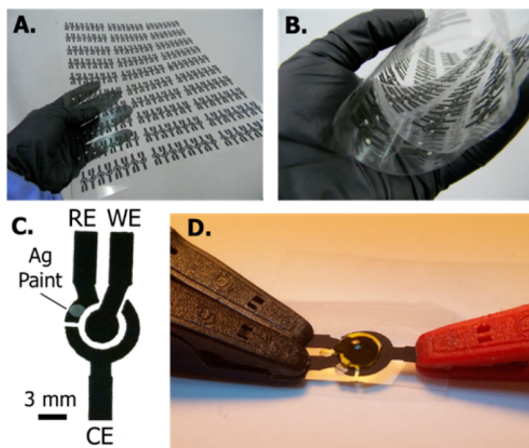


**Figure 2.** SPCEs on transparency film shown as (A) printed sheet that is (B) flexible. (C) A single printed electrode image (with background removed for visualization) showing working (WE), silver paint reference (RE), and counter (CE) electrode geometries and connections. (D) Final device image with 30  $\mu$ L of solution contained within the central well and connected to potentiostat leads.

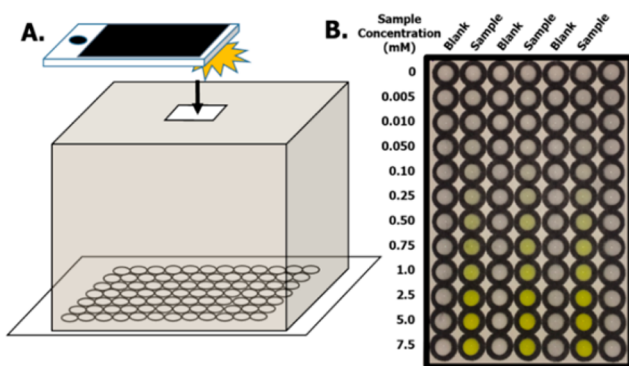


**Figure 3.** Scheme showing (A) the image capture process using a cellphone for the “light box” plate reading method and resulting (B) PNP calibration image labeled with blank and sample regions.

flash intensity across the device, the light controls were used to normalize the brightness to give more precise results. More detailed explanation of image analysis can be found in the [Supporting Information](#).

**Electrochemical Detection of PNP, ONP, and PAP.** Electrochemical detection of PNP, ONP, and PAP was performed using square wave voltammetry (SWV). Optimal parameters for amplitude, frequency and step height were determined for each species to be PNP (amplitude, 50 mV; frequency, 50 Hz; step height, 5 mV), ONP (amplitude, 55 mV; frequency, 60 Hz; step height, 5 mV), PAP (Amplitude: 75 mV, Frequency: 60 Hz, Step Height: 5 mV). Buffer and pH optimization was performed using phosphate-buffered saline (PBS), phosphate-citrate buffered saline (PCS buffer), and carbonate buffered saline all with 0.4 M KCl background electrolyte. Different pH buffers were made by adjusting the ratio of acid/base pairs; PBS buffers used 0.2 M  $\text{KH}_2\text{PO}_4$  and  $\text{Na}_2\text{HPO}_4$ , PCS buffers used 0.2 M  $\text{Na}_2\text{HPO}_4$  and 0.1 M citric acid monohydrate, carbonate buffer used 0.2 M  $\text{Na}_2\text{CO}_3$  and  $\text{NaHCO}_3$ . Final pH values for each buffer were read using a pH meter. Further buffer recipe details can be found in the [Supporting Information](#).

**Enzymatic Assay Optimization.** Enzymatic assay optimization was performed spectrophotometrically for ONP and PNP producing reactions within 96-well plates and read using a microtiter plate reader. Each well contained a total reaction volume of 200  $\mu$ L, and reactions were quenched by adding 0.5 M NaOH to the sample (0.25 M NaOH final concentration). Detection was done under basic conditions to inactivate the enzyme and also ensure the product was in its anionic form. PNP and ONP are colorless below and yellow above their  $\text{pK}_a$  values (pH 7.18 and 7.23, respectively). ONP and PNP production was detected at 400 nm. Detection of PAP was performed electrochemically using optimized parameters using SPCEs on the transparency film.  $\beta$ -gal activity was detected using the following substrates: PNP-gal, ONP-gal, or PAP-gal.  $\beta$ -glucr activity was detected using PNP-glucr.  $\beta$ -gluco was detected using PNP-Gluc or ONP-Gluc. With each of these substrates, the carbohydrate moiety is cleaved off by the enzyme leaving either PAP, PNP, or ONP as the product. The optimal reaction pH/buffer of each enzyme was determined using PCS buffer of pH 3–7.5 for  $\beta$ -gluco or PBS of pH 5.5 to 9 for both  $\beta$ -glucr and  $\beta$ -gal. Optimal pH for  $\beta$ -gal,  $\beta$ -glucr, and  $\beta$ -gluco were determined to be pH 7.5 PBS, pH 6.5 PBS, pH 5.5 PCS buffers, respectively.

**Bacterial Detection.** The bacterial strains included pathogenic *Escherichia coli* O157:H7 PTVS016 (lettuce-associated outbreak isolate obtained from human feces) and *E. coli* O157:H7 PTVS087 (lettuce isolate possibly linked to an outbreak); *Enterococcus faecalis* BB1172 and *E. faecium* BB498 (wild-type strains isolated from concentrated animal feeding operations); as well as nonpathogenic *E. coli* P14 (ATCC BA-1430) and *E. coli* P68 (ATCC BA-1431) originating from cattle hides. Probe sonication was compared to chemical lysing using an optimal 20 s for cell lysing and a 50:50 solution of 10% chloroform and 0.005% SDS for chemical lysing prior to performing enzymatic assays.

Detection of low concentrations of pure bacterial cultures was conducted using dilutions of pure cultures at stationary phase (18–24 h old) incubated in media with 1 mL aliquots taken for enzymatic assay testing. For food and water samples, alfalfa sprouts were purchased from Whole Foods and unfiltered water was obtained from Colorado State University’s Lagoon (latitude, 40.57566; longitude, -105.08631; elevation, 1523 m; date, 02/08/2016; outdoor temperature, -1.7 °C) and both were stored in the refrigerator at 4 °C overnight (10 h) prior to testing. Inoculated water and sprout samples contained  $2.3 \times 10^2$  and  $3.1 \times 10^1$  CFU/g of *E. coli* and *E. faecalis*, respectively. For food samples and water samples, 10 g or 10 mL of sample (inoculated or uninoculated control) alfalfa sprouts or lagoon water, respectively, were mixed with 90 mL of BHI media. Sprout-media mixtures were placed in a stomacher mixer for 1 min to mix/wash the sprouts. Water-media solutions were hand mixed to ensure a homogeneity. All samples were incubated in a 37 °C shaker incubator with shaking at 100 rpm, sampled at set time intervals, and then sonicated (1 mL for 30 s at 5 W). Assays were reacted in centrifuge tubes with 250  $\mu$ L of sonicated sample and 250  $\mu$ L of substrate and buffer. After 1 h, 250  $\mu$ L of 0.5 M NaOH in 0.4 M KCl was added to stop the reaction and the final solution was analyzed for both colorimetric and electrochemical measurements. Spread plating following serial dilutions was performed to determine inoculum levels in CFU/mL.

## RESULTS AND DISCUSSION

**Optimizing Electrochemical Detection.** Several factors were considered when optimizing the electrode platform. Initially, inexpensive copy paper and Whatman 1 filter paper were studied as substrate materials for electrochemical detection. A model inner-sphere electron transfer species,  $K_3Fe(CN)_6/K_4Fe(CN)_6$ ,<sup>48</sup> was used to determine carbon electrode platform performance (Figure S3). Scan rate studies performed indicated that copy paper provided the poorest performance, with lower peak currents (anodic  $i_p = 123 \pm 7 \mu A$  at 100 mV/s) and higher peak spitting ( $\Delta E_p = 278 \pm 3$  mV at 100 mV/s) relative to Whatman 1 filter paper (anodic  $i_p = 147 \pm 13 \mu A$ ,  $\Delta E_p = 206 \pm 8$  mV at 100 mV/s). Poly(ethylene terephthalate) (PET) transparency film sheets were also studied. Because transparency film is nonporous and the carbon ink is slightly hydrophobic, the electrode geometry itself created a barrier that was maintained by solution surface tension without the need for an additional wax barrier. Transparency film-based electrodes provided similar electrochemical performance (anodic  $i_p = 145 \pm 2 \mu A$ ,  $\Delta E_p = 223 \pm 1$  mV at 100 mV/s) to electrodes printed on filter paper but with lower standard deviations. This is similar to a previously reported study by Banks et al. using tracing paper and is likely due to the more consistent electrode area and solution contact when compared with paper substrates.<sup>49</sup> While Whatman filter-based electrodes provided the best results for fully paper-based devices, a small interference peak ( $\sim 850$  mV) was discovered in the background cyclic voltammetry scans at potentials that overlapped with PNP and ONP oxidation peaks (Figure S4). The peak also appeared when using copy paper as the substrate for electrodes. While the species giving rise to the signal is unknown at present, it might be possible that if the paper were soaked and rinsed, the interference could be removed; however, this would need to be further studied for confirmation. Given transparency film electrodes did not produce background peaks and were inexpensive (\$0.006/device) and easier to fabricate, they were used throughout the remaining experiments.

Next, transparency film electrodes were used to characterize the electrochemical behavior of PAP, ONP, and PNP. PAP has been studied for the direct electrochemical detection of bacterially produced enzymes, while ONP and PNP have not been studied.<sup>50</sup> ONP and PNP can either be reduced via a  $6e^-$  transfer process or oxidized via a  $1e^-$  transfer process.<sup>51-54</sup> While reduction offers a higher molar electron transfer, the enzymatic substrates also produced a background reduction peak at the same potential ( $-700$  mV vs Ag/AgCl). The oxidation reaction was therefore selected for further study. It is of note, however, that product formation of PNP and ONP does create a significant increase in peak current above the substrate reduction background peak due to the higher rate of electron transfer per mole of product produced and remains an alternative option for detection. Figure 4 shows the detection calibration for PNP, ONP, and PAP using optimized SWV conditions. Detection limits for PNP, ONP, and PAP were calculated to be 1.1, 2.8, and  $0.5 \mu M$  (3SD/slope) with linear ranges for all three reactions determined to be  $25-500 \mu M$ . As expected for a  $2e^-$  transfer process, PAP has approximately doubled the peak height of the  $1e^-$  transfer process of PNP and ONP.

**Colorimetric Detection Optimization.** Similar to previously described work that used a flat-bed scanner for reading 96-well plates,<sup>44</sup> we developed a simple and inexpensive

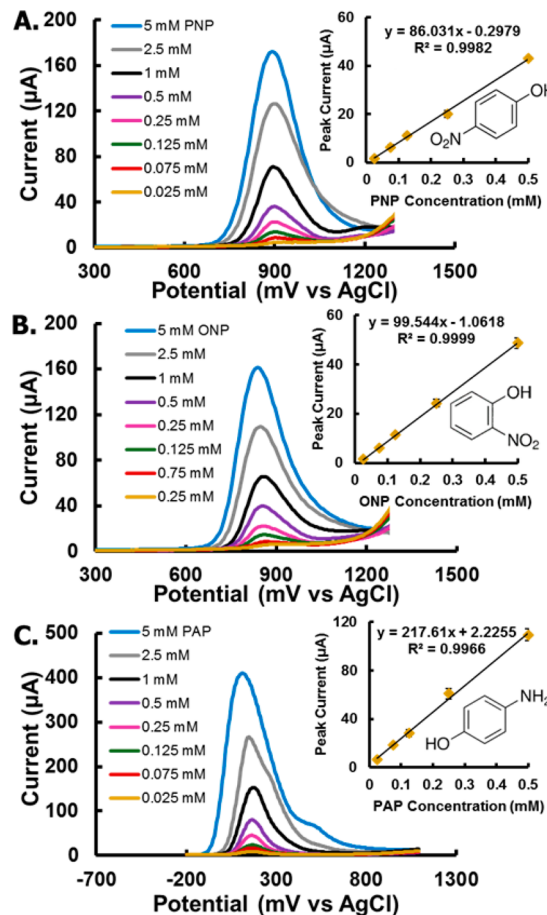


**Figure 4.** Optimal SWV settings used to measure and plot increasing concentrations of (A) PNP, (B) ONP, and (C) PAP detection along with the resulting linear range calibration plots in pH 6.5 PBS buffer ( $n = 3$ ).

detection scheme to take the place of a plate reader for paper-based detection. A cell phone camera was used to both image and wirelessly send results for analysis. Analysis of allowed for measurements to be taken as a function of time (Figure 3). The method is an improvement to our previously described method for bacteria detection, where results were only acquired once the device dried.<sup>22,55,56</sup> We also studied the use of standards on either side of each spot test to normalize the background lighting and solution conditions. Figure 3 and Figure S2 show the process of image analysis and normalization. Using the light box and background normalization method, the detection limit for ONP was decreased from  $151 \mu M$  to  $81 \mu M$  for ONP (Figure S5) and from  $260 \mu M$  to  $119 \mu M$  for PNP detection. Figure S5 shows the decrease in average relative standard deviations with normalization from 28% to 9.2% over the linear range (0.1–1 mM). While the detection limit is higher than that of a plate reader (4.4  $\mu M$  and 9.6  $\mu M$  for ONP and PNP, respectively), the portability is improved and cost is significantly reduced. Part of the increase in detection limit is due to the decrease in path length on paper when compared to the plate reader. While the electrochemical detection of PNP has been reported using ePADs,<sup>57</sup> to the best of our knowledge only the colorimetric detection of PNP and not ONP has been reported with PADs.<sup>58</sup> Murdock et al. used alkaline phosphatase as a tag in enzyme-linked immunosorbent assays (ELISAs) in paper-based wells to react with *p*-

nitrophenyl phosphate (PNPP) and form PNP. While similar, this method only calibrated a dried, end-point color intensity with respect to antigen concentration.

**Enzyme Detection Optimization.** Once optimal electrochemical and colorimetric parameters were established for each reaction, enzymatic conditions were optimized. Each enzymatic reaction was optimized using pure enzyme dilutions. Aside from PAP-gal assay detection, which was conducted electrochemically, colorimetric detection was done to optimize all other assays. Optimal pH conditions for the highest activity were achieved for  $\beta$ -gluco in pH 5.5 Phosphate-citrate buffer (Figure S6A)  $\beta$ -gal in pH 7.5 PBS (Figure S6B),  $\beta$ -glucr in pH 6.5 PBS. Optimal substrate concentrations for 1 U/mL of enzyme (representative of a high concentration of bacteria) were determined by varying substrate concentrations. With *E. coli* enzymes, peak signal response was reached for  $\beta$ -gal at 2.5 mM for ONP-gal, PNP-gal, and PAP-gal substrates, while  $\beta$ -glucr peaked at 2 mM PNP-gluco (Figure S7). *Enterococcus* spp. enzyme  $\beta$ -gluco provided a maximum signal at 7.5 mM for PNP-gluco and 10 mM for ONP-gluco (Figure S7). All reactions developed the highest color change after one h with the exception of ONP-gal and ONP-gluco both of which peak in signal within 10 min (Figure S7). Beyond 1 h, evaporation from the paper-based wells began to significantly change signal response.

Detection limits for each enzyme/substrate pair were conducted using optimal substrate concentrations. Enzyme LODs obtained for PNP-gluco (0.2  $\mu$ g/mL), ONP-gluco (2  $\mu$ g/mL), PNP-glucr (7  $\mu$ g/mL), PNP-gal and ONP-gal were both about 1.5  $\mu$ g/mL. Differences in LOD and optimal substrate concentrations for the same enzyme but different substrates are a result of substrate affinity and possible feedback inhibition effects.<sup>59</sup> The high relative detection limit for PNP-gluco is probably due to substrate inhibition, which occurs in approximately 20% of enzymes.<sup>60</sup> While most substrate optimization curves were logarithmic, the signal for PNP-gluco (Figure S7) decreased above 2 mM until almost no activity was measurable at 10 mM. When testing PNP-gluco with bacteria, it also gave the lowest signal, which could also be indicative of substrate inhibition or lower  $\beta$ -glucr expression.

**PNP vs ONP Substrates.** A comparison between the use of PNP and ONP substrates for  $\beta$ -gluco found that PNP-gluco produced a significantly higher signal than ONP-gluco. As such, ONP-gluco was not used in the final experiments involving *Enterococcus* spp. For  $\beta$ -gal, ONP-gal reacted faster than PNP-gal; however, over longer reaction times, PNP-gal provided a higher signal on the plate reader and paper. Because ONP and PNP demonstrate similar molar absorptivity, this is likely due to increased reaction efficiency with  $\beta$ -gal and PNP-gal compared with ONP-gal.

An interesting phenomenon occurred when ONP assays reacted in the paper-based wells for more than 10 min. A noticeable decrease in signal occurred within the sample wells, while simultaneously the light control spots and surrounding paper began to turn yellow. This phenomenon was not observed within the deeper wells of the plate reader or for PNP assays on paper. This was determined to be due to the higher vapor pressure of ONP (12 Pa) relative to the vapor pressure of PNP (0.32 Pa) resulting in gas phase transfer between spots.<sup>61</sup> The high vapor pressure is in part due to the ortho-position of the hydroxyl group, which causes ONP to form intramolecular hydrogen bonding and decreases intermolecular hydrogen bonding, contributing to its volatility. Because of ONP's

comparatively high volatility, it would not be practical to react ONP in open PAD devices. When detecting bacteria, therefore, the reactions were completed in microfuge tubes before being quantified on paper so that ONP could be used for detecting bacteria.

**Bacterial Detection.** Given the need to enrich bacteria after sampling to verify cell viability, we next considered the impact of growth media on both colorimetric and electrochemical signals. We first studied removing culture media and resuspending cells in buffer to remove the colored background and potential electrochemical interferences as well as provide a simple preconcentration step. Figure 5A shows the electro-

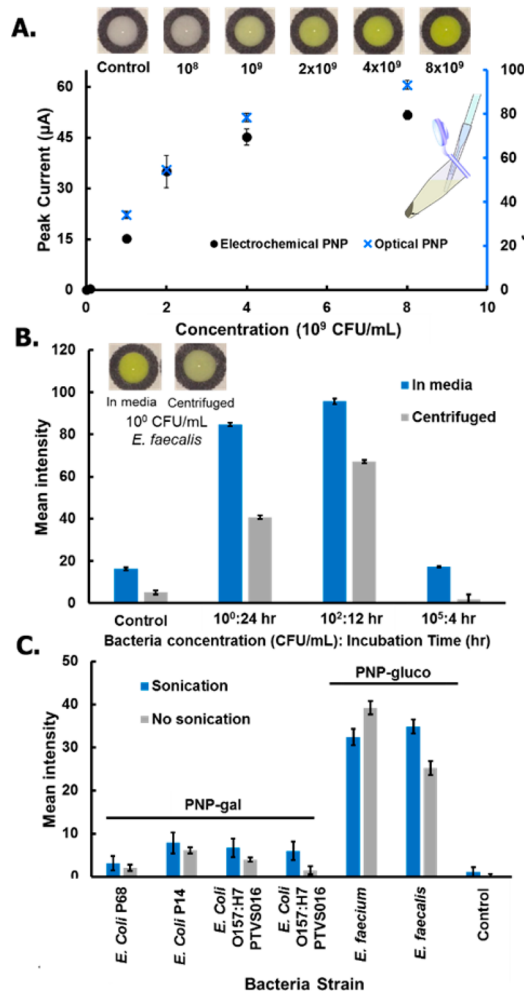


**Figure 5.** Showing (A) electrochemical and colorimetric response of centrifuged and resuspended *E. faecalis* incubated for 2 h with PNP-gluco substrate and (B) comparison of the same strain and reaction in media vs centrifuged with increasing concentrations and decreasing assay time. (C) Comparison of 20 s of sonication for all tested bacteria strains with their corresponding PNP substrates for  $\beta$ -gal for *E. coli* and  $\beta$ -glucr for enterococci ( $n = 3$ ). Controls include reaction well without bacteria present.

chemical and colorimetric detection of PNP-gluco with resuspension of cells after media removal. It was found, however, that keeping the cells in their original media gave higher colorimetric signals than centrifuging and resuspending cells in buffer (Figure 5B). This is due to either loss of secreted enzymes during centrifuging or possibly the natural release and buildup of enzyme within the media due to cell death and

apoptosis over time before centrifuging. When removing the media, enzymes were removed as well. In an attempt to regain enzymatic activity, we explored chemical and probe sonication-based lysing methods that we have previously shown enhanced detection. The 20 s of probe sonication provided the highest intensity signal over no lysing for the majority of bacteria species detected (Figure 5C). Chemical lysing, however, resulted in no assay response, likely due to the enzyme denaturation by the chloroform or SDS. While sonication with media removal is a viable option for measuring enzyme activity within cells, the current study utilized the direct sonication and detection of bacteria within media due to its simpler preparation and higher signal.

Using electrochemical detection, an interference peak was found at the same potential that both PNP and ONP oxidation occur. While this was initially thought to be an issue, it was determined that increasing the detection pH removed the peak from the solvent window background. Because of its complex composition, it is unclear what media component(s) oxidize at this potential; however, it has been hypothesized to be associated with phenolic molecules, such as tyrosine.<sup>62</sup> The oxidative peak current for PNP and ONP showed little change with increasing pH up to pH 10.5, and Figure S8 shows the electrochemical peak current for PNP, ONP, and PAP with pH. The same concentration of NaOH (0.5 M) that is used in the colorimetric detection of PNP and ONP was found to be optimal for peak removal. Therefore, the same solutions used for colorimetric detection could also be used for electrochemical detection. PAP did not suffer from the same interference, however, and due to its chemical sensitivity to pH was detected directly.

Bacterial strains used as indicators of fecal contamination in food and water, *E. coli* and *Enterococcus* spp. were tested from pure cultures to assess assay performance and time to detection. For both electrochemical and colorimetric detection, none of the bacterial strains tested developed signals at 4 h, which is not surprising given the low starting concentrations of bacteria, but all  $10^1$  CFU/mL dilutions produced signals by 8 h (Figure 6). By 12 h, a maximum signal had been obtained for all bacterial strains and dilutions, except for both colorimetric and electrochemical detection of PNP-gluco for *E. faecium* and all colorimetric assays for *E. coli* PTVS087, both of which generated maximum signal at 18 h. However, as discussed below, a decrease was seen in the colorimetric *Enterococcus* spp. assays at 24 h that was further mimicked for only one strain, *E. faecalis*, with electrochemical detection. The assay results for PNP-gluco detection were omitted, because these pathogenic strains are negative for  $\beta$ -glucuronidase production and all time points were negative. Therefore, using this assay is one way pathogenic strains of *E. coli* O157:H7 are identified. Interestingly, it was determined that ONP substrates provided higher signals than PNP substrates for colorimetric detection; however, the opposite can be seen for electrochemical detection. The heat map in Figure 6 emphasizes these differences where darker colors indicate more formation of PNP and ONP products for both colorimetric and electrochemical detection. This is probably due to the slightly lower and higher detection limits for ONP colorimetric and electrochemical detection, respectively.

**Food and Water Sample Testing.** Detection of foodborne pathogens requires a sampling and culture technique appropriate for the manner of contamination that might occur. Our previous studies used a swabbing technique to detect

CFU/mL			Electrochemical ( $\mu$ A)					Colorimetric (Mean Intensity)				
			Time (hr)					Time (hr)				
			4	8	12	18	24	4	8	12	18	24
<i>E. coli</i> P14	PNP-gal	10 <sup>1</sup>	-	63.17	73.10	84.70	61.67	-	67.93	84.21	83.11	63.71
		10 <sup>2</sup>	-	59.77	96.63	100.42	97.03	-	64.38	102.25	86.88	90.30
		10 <sup>3</sup>	-	65.20	103.33	93.92	90.20	-	71.13	103.17	85.18	89.13
	ONP-gal	10 <sup>1</sup>	-	42.21	62.97	74.90	89.53	-	51.04	113.10	98.91	103.89
		10 <sup>2</sup>	-	43.91	71.20	72.17	81.40	-	49.00	114.35	99.94	107.28
		10 <sup>3</sup>	-	57.10	68.30	82.00	88.00	-	67.47	112.28	99.14	107.69
	PNP-Gluc	10 <sup>1</sup>	-	75.30	70.28	64.89	78.21	-	73.32	76.45	65.65	72.48
		10 <sup>2</sup>	-	68.80	76.85	65.29	76.68	-	67.80	78.28	67.18	71.58
		10 <sup>3</sup>	-	69.87	75.53	68.90	76.83	-	70.05	77.86	65.31	72.79
<i>E. coli</i> O157:H7	PNP-gal	10 <sup>1</sup>	-	22.03	114.30	107.26	115.30	-	27.34	79.93	106.45	106.94
		10 <sup>2</sup>	-	66.87	115.17	113.90	113.80	-	72.76	82.42	108.13	109.31
		10 <sup>3</sup>	-	70.57	121.93	113.23	114.83	-	73.13	81.61	109.63	109.28
	ONP-gal	10 <sup>1</sup>	-	17.08	77.13	81.13	76.73	-	21.37	84.79	116.11	117.41
		10 <sup>2</sup>	-	45.72	68.23	78.50	74.23	-	63.05	85.16	116.16	118.37
		10 <sup>3</sup>	-	59.25	75.90	80.89	78.47	-	75.45	85.70	116.90	117.53
	PNP-gluc	10 <sup>0</sup>	-	-	93.03	103.55	103.45	-	-	106.04	104.37	84.37
		10 <sup>1</sup>	-	5.50	117.17	111.93	95.29	-	6.67	108.70	102.83	85.75
		10 <sup>2</sup>	-	36.02	95.50	88.60	83.05	-	44.00	96.92	90.76	77.28
<i>E. faecium</i> <i>E. faecalis</i>	PNP-gluc	10 <sup>0</sup>	-	-	19.74	20.40	68.05	-	-	20.72	14.35	66.24
		10 <sup>1</sup>	-	4.22	22.83	76.85	79.07	-	6.47	38.04	91.97	70.16
		10 <sup>2</sup>	-	33.34	27.50	79.87	83.78	-	42.17	41.96	90.18	75.42

**Figure 6.** Heat map showing average ( $n = 3$ ) measured colorimetric normalized mean intensity (AU) and electrochemical peak current ( $\mu$ A) detection of PNP and ONP production from enzymatic assays measured after 1 h of reaction. Each strain was tested for three dilutions at low concentrations (CFU/mL), cultured, and measured with pre-enrichment culture time (— indicates signals below the detection limit).

surface contamination on ready-to-eat and butcher meats.<sup>21,63</sup> However, for large surface area foods such as leafy greens, a washing/mixing technique is preferable, as was previously demonstrated for bacterial detection from spinach leaves.<sup>63</sup> Raw sprouts were inoculated with a generic *E. coli* species (P14) and *Enterococcus faecalis* to simulate contaminated food and sampled using a washing/mixing approach. Figure 7 shows the resulting colorimetric and electrochemical detection of cultured sprouts as a function of time. For both detection methods there was not a significant difference between raw and inoculated sprouts except for colorimetric detection of  $\beta$ -galactosidase activity at 4, 18, and 24 h in which there is a slightly higher

C/I			Electrochemical ( $\mu$ A)					Colorimetric (Mean Intensity)				
			Time (hr)					Time (hr)				
			4	8	12	18	24	4	8	12	18	24
Sprouts	PNP-gal	C	9.70	84.82	60.40	59.90	51.63	16.59	78.82	82.36	88.68	73.28
		I	18.70	77.16	64.07	49.90	47.69	27.6	80.81	82.24	108.35	103.37
		C	15.67	65.98	58.60	48.80	60.77	20.14	95.78	102.37	88.88	79.55
	ONP-gal	I	22.65	63.70	53.47	41.33	44.29	35.64	95.99	99.87	107.36	102.79
		C	50.50	73.43	49.70	45.87	51.17	63.00	76.30	69.96	75.25	75.56
		I	58.73	91.37	59.39	39.83	37.13	65.13	76.87	80.79	78.78	75.30
	PNP-Gluc	C	-	-	-	-	-	-	-	-	-	-
		I	-	53.97	102.6	83.73	74.55	-	69.06	111.79	111.33	101.87
		C	-	-	-	-	-	-	-	-	-	-
Water	ONP-gal	I	-	36.23	52.51	50.3	50.31	-	62.09	117.30	120.78	111.25
		C	-	74.63	59.05	46.93	44.77	-	43.64	81.81	83.91	84.27
	PNP-Gluc	I	-	82.48	61.97	53.67	46.97	-	75.13	104.11	88.37	78.55
		C	-	-	-	-	-	-	-	-	-	-

**Figure 7.** Electrochemical peak current and colorimetric measured mean gray intensity for inoculated (I) and control (C) sprout and water samples measured with increasing pre-enrichment culture time. Assay time 1 h. (— indicates signals below the detection limit ( $n = 3$ )).

intensity signal for the inoculated sprout samples. In addition, electrochemistry also detected a slight increase with inoculation for  $\beta$ -gluco activity at 4, 8, and 12 h time points. Without inoculation, the sprouts contained  $1.5 \times 10^9$  CFU/g of bacteria, as verified by culture methods (spread plating). The lack of differences between control and inoculated sprout samples is probably due to the very high initial concentration of bacteria, where, except at initial time points, the enzyme assays quickly reached a saturation point. Neither colorimetric, nor electrochemical detection found  $\beta$ -glucr activity in the raw or inoculated sprouts. This high initial concentration could also have inhibited enzyme production or cell growth of the inoculated  $\beta$ -glucr expressing bacteria, which can occur with mixed bacterial growth due to competitive behavior and cellular signaling responses.<sup>64</sup> While  $\beta$ -glucr was negative, all  $\beta$ -gal assays achieved positive signal within 4 h, emphasizing the need for multiple assays when determining FIB contamination.

For model irrigation water sample detection, no signal was obtained with lagoon water samples without inoculation. The lagoon water had a significantly lower bacterial concentration at  $2.9 \times 10^2$  CFU/mL when compared to sprouts. In this case, the species of bacteria present probably did not express the target enzymes employed and were therefore probably not FIB since concentrations were low enough that inhibition effects are significantly less likely. Inoculated bacteria were detected by all assays for both colorimetric and electrochemical detection within 8 h. Because of the low concentrations of bacteria found in water ( $<10^2$  CFU/mL), filtration steps are usually taken to reduce analysis and culture time while improving detection limits.<sup>65</sup> While we did not use filtration, we have previously demonstrated the use of an inexpensive and portable pump and filter device known as a Modified Moore Swab (MMS) to improve sensitivity by filter collection and low bacteria concentration detection ( $\sim 10^{-1}$  CFU/mL) from large amounts of water.<sup>66,67</sup>

While colorimetric and electrochemical detection of food and water samples produced similar results, a few key differences were noted. As discussed previously for pure culture studies, while ONP-gal presented higher signal for colorimetric detection than PNP-gal, the opposite was true for electrochemical detection. An interesting phenomenon occurred with the electrochemical detection studies. Starting at 12 h, the electrochemical signal for all sprout sample assays decreased. This behavior was also seen in inoculated water samples, where a decrease in all assays except ONP-gal, starting at 18 h for PNP-gal, and 12 h for both PNP-gluco and PNP-glucr. This decrease in signal was also measured by colorimetric detection at 24 h for all assays except PNP-glucr, which occurred at 18 h. We have two hypotheses to why this is occurring. The first could be associated with changes in pH of the media or other interfering metabolites being produced by the bacteria over time. Measured changes in cell culture for all strains grown from  $\sim 10^5$  CFU/mL went from pH 7.5 to 5.5 after 12 h. While both *Enterococcus* strains remained relatively low at  $\sim$ pH 6, the *E. coli* strains increased back up to  $\sim$ pH 7. This could affect enzymatic reaction rates and possibly measured assay intensities. The second hypothesis could be that the phenomenon is associated with cell growth and the expression of enzymes. Although it is not yet known what causes the decrease in signal, it was found that both assays perform nearly equally as well. The electrochemical detection assay does offer an alternative method for detection that is not interfered with by solution color and/or scattering.

For comparison purposes, Figure S9 shows the assay results for  $\beta$ -gal detection using PAP-gal assays. Not all time points were measured with this assay due to time constraints. Although PAP is a  $2e^-$  process, it does not always produce a higher current response than PNP or ONP within these assay conditions. In fact, of the time points that can be compared, only the 12 h time point for *E. coli* P14 and all time points for *E. coli* PTVS087 were higher in signal. However, this current is significantly lower than would be expected for an undiluted and a  $2e^-$  current reaction (compared to  $1e^-$  reaction diluted in half with base for PNP and ONP assays). Compared to the real samples tested, PAP-gal also generated a significantly lower current response when measuring the sprout assays when compared with ONP-gal and PNP-gal for all time points tested. Significant decreases in peak currents were measured at 24 h, and this along with the wide degree of signal variability with sample, indicate that PAP is possibly more prone to degradation and/or environmental effects when testing bacteria.

## CONCLUSIONS

Herein, we have developed procedures for the detection of FIB bacteria using colorimetric and electrochemical detection within paper-based wells and transparency-film based electrochemical cells. Both methods can use the same assays for detection and future device development could couple detection platforms for more simple yet comprehensive analysis using both techniques. The advantages of using both methods can overcome disadvantages associated with using an individual technique, making a combined approach more applicable to a wider range of sample types and applications. Both methods successfully measured the presence of FIB enzyme activity in inoculated food and water samples. While electrochemical detection did not offer a substantial decrease in detection time relative to the colorimetric method, more time points are needed to verify this outcome. Without modification, electrochemistry offered similar detection limits to the plate reader, which is an order of magnitude below the paper-based colorimetric method. This study serves as a basis for further development as there remain many opportunities for improving electrochemical detection that would make the electrode substantially more sensitive than the standard colorimetric approaches. One method proposed by Hernández et al. would be in adding an electrochemical/chemical preconcentration step.<sup>68</sup> Both ONP and PNP have been successfully separated from background solutions and into the electrode itself via the inclusion of a C<sub>18</sub> chromatography powder within a carbon paste electrode matrix. Limits of determination (mean  $\pm 10$  SD) for ONP and PNP using this method were  $1.4 \times 10^{-8}$  and  $3.1 \times 10^{-8}$  M, respectively, which is 3 and 2 orders of magnitude below the ONP and PNP LOD measurements we obtained by the smart phone method and traditional plate reader, respectively. One way to improve detection limits for both assays is to use inducers to increase enzyme expression in cultured cells.<sup>45</sup> Isopropyl- $\beta$ -D-thiogalactopyranoside (IPTG) and methyl- $\beta$ -D-glucuronide (MetGlu) have been used to induce  $\beta$ -Gal and  $\beta$ -glucr expression, respectively. Further optimization of both electrochemical and colorimetric assays and their detection platforms would provide improved detection of food and water bacterial contamination.

## ASSOCIATED CONTENT

### Supporting Information

The Supporting Information is available free of charge on the ACS Publications website at DOI: [10.1021/acs.analchem.6b05009](https://doi.org/10.1021/acs.analchem.6b05009).

Further information on materials and methods, colorimetric detection process, electrochemical device characterization and optimization, assay optimization, and colorimetric and electrochemical bacterial studies ([PDF](#))

## AUTHOR INFORMATION

### Corresponding Author

\*E-mail: [Chuck.Henry@colostate.edu](mailto:Chuck.Henry@colostate.edu). Phone: +1-970-491-2852.

### ORCID

Charles S. Henry: [0000-0002-8671-7728](https://orcid.org/0000-0002-8671-7728)

### Notes

The authors declare no competing financial interest.

## ACKNOWLEDGMENTS

The authors gratefully acknowledge funding from grants through the U.S. Department of Agriculture (USDA, Grant 16-7400-0859-CA) and the National Institutes of Health (Grant R01OH010662). Additional support for this work was provided by Colorado State University through the Catalysts for Innovative Partnerships program. The authors also thanks Dr. B. Geiss for useful discussions regarding bacterial detection.

## REFERENCES

- (1) CDC. *Surveillance for Foodborne Disease Outbreaks—United States, 2009–2010*; MMWR, 2013.
- (2) CDC. *Surveillance for Waterborne Disease Outbreaks Associated with Drinking Water—United States, 2011–2012*; MMWR, 2015.
- (3) Uyttendaele, M.; Jaykus, L.-A.; Amoah, P.; Chiodini, A.; Cunliffe, D.; Jacxsens, L.; Holvoet, K.; Korsten, L.; Lau, M.; McClure, P.; Medema, G.; Sampers, I.; Rao Jasti, P. *Compr. Rev. Food Sci. Food Saf.* **2015**, *14*, 336–356.
- (4) Steele, M.; Odumeru, J. *J. Food Prot.* **2004**, *67*, 2839–2849.
- (5) Painter, J. A.; Hoekstra, R. M.; Ayers, T.; Tauxe, R. V.; Braden, C. R.; Angulo, F. J.; Griffin, P. M. *Emerging Infect. Dis.* **2013**, *19*, 407–415.
- (6) Crowe, S. J.; Mahon, B. E.; Vieira, A. R.; Gould, L. H. *MMWR. Morbidity and mortality weekly report* **2015**, *64*, 1221.
- (7) Harwood, V. J.; Staley, C.; Badgley, B. D.; Borges, K.; Korajkic, A. *FEMS Microbiology Reviews* **2014**, *38*, 1–40.
- (8) Silva, N.; Igrefas, G.; Gonçalves, A.; Poeta, P. *Ann. Microbiol.* **2012**, *62*, 449–459.
- (9) Odonkor, S. T.; Ampofo, J. K. *Microbiol. Res.* **2013**, *4*, 2.
- (10) Scott, T. M.; Jenkins, T. M.; Lukasik, J.; Rose, J. B. *Environ. Sci. Technol.* **2005**, *39*, 283–287.
- (11) Boehm, A. B.; Sassoubre, L. M. *Enterococci as Indicators of Environmental Fecal Contamination*; Massachusetts Eye and Ear Infirmary: Boston, MA, 2014.
- (12) Gorbach, S. L. *Microbiology of the Gastrointestinal Tract*, 4th ed.; University of Texas Medical Branch at Galveston: Galveston, TX, 1996; Chapter 95.
- (13) FDA.
- (14) Lazcka, O.; Campo, F. J. D.; Muñoz, F. X. *Biosens. Bioelectron.* **2007**, *22*, 1205–1217.
- (15) Wang, Y.; Salazar, J. K. *Compr. Rev. Food Sci. Food Saf.* **2016**, *15*, 183–205.
- (16) Banada, P. P.; Bhunia, A. K. In *Principles of Bacterial Detection: Biosensors, Recognition Receptors and Microsystems*; Zourob, M., Elwary, S., Turner, A., Eds.; Springer: New York, 2008; pp 567–602.
- (17) Gonzalez, R. A.; Noble, R. T. *Water Res.* **2014**, *48*, 296–305.
- (18) Rhoads, D. D.; Wolcott, R. D.; Sun, Y.; Dowd, S. E. *Int. J. Mol. Sci.* **2012**, *13*, 2535–2550.
- (19) Cate, D. M.; Adkins, J. A.; Mettakoonpitak, J.; Henry, C. S. *Anal. Chem.* **2015**, *87*, 19–41.
- (20) Yetisen, A. K.; Akram, M. S.; Lowe, C. R. *Lab Chip* **2013**, *13*, 2210.
- (21) Jokerst, J. C.; Adkins, J. A.; Bisha, B.; Mentele, M. M.; Goodridge, L. D.; Henry, C. S. *Anal. Chem.* **2012**, *84*, 2900.
- (22) Bisha, B.; Adkins, J. A.; Jokerst, J. C.; Chandler, J. C.; Pérez-Méndez, A.; Coleman, S. M.; Sbodio, A. O.; Suslow, T. V.; Danyluk, M. D.; Henry, C. S.; Goodridge, L. D. *J. Visualized Exp.* **2014**, e51414.
- (23) Li, C.-z.; Vandenberg, K.; Prabhulkar, S.; Zhu, X.; Schnepel, L.; Methee, K.; Rosser, C. J.; Almeida, E. *Biosens. Bioelectron.* **2011**, *26*, 4342–4348.
- (24) Hossain, S. M.; Ozimok, C.; Sicard, C.; Aguirre, S. D.; Ali, M. M.; Li, Y.; Brennan, J. D. *Anal. Bioanal. Chem.* **2012**, *403*, 1567–1576.
- (25) Wang, Y.; Ping, J.; Ye, Z.; Wu, J.; Ying, Y. *Biosens. Bioelectron.* **2013**, *49*, 492–498.
- (26) Struss, A.; Pasini, P.; Ensor, C. M.; Raut, N.; Daunert, S. *Anal. Chem.* **2010**, *82*, 4457–4463.
- (27) Park, T. S.; Li, W.; McCracken, K. E.; Yoon, J. Y. *Lab Chip* **2013**, *13*, 4832–4840.
- (28) Rattanarat, P.; Dungchai, W.; Cate, D.; Volckens, J.; Chailapakul, O.; Henry, C. S. *Anal. Chem.* **2014**, *86*, 3555–3562.
- (29) Dungchai, W.; Chailapakul, O.; Henry, C. S. *Anal. Chem.* **2009**, *81*, 5821–5826.
- (30) Nie, Z.; Deiss, F.; Liu, X.; Akbulut, O.; Whitesides, G. M. *Lab Chip* **2010**, *10*, 3163–3169.
- (31) Adkins, J.; Boehle, K.; Henry, C. *Electrophoresis* **2015**, *36*, 1811–1824.
- (32) Mettakoonpitak, J.; Boehle, K.; Nantaphol, S.; Teengam, P.; Adkins, J. A.; Srisa-Art, M.; Henry, C. S. *Electroanalysis* **2016**, *28*, 1420.
- (33) Tschirhart, T.; Zhou, X. Y.; Ueda, H.; Tsao, C.-Y.; Kim, E.; Payne, G. F.; Bentley, W. E. *ACS Synth. Biol.* **2016**, *5*, 28–35.
- (34) Baldrich, E.; Muñoz, F. X.; García-Aljaro, C. *Anal. Chem.* **2011**, *83*, 2097–2103.
- (35) Pérez, F.; Tryland, I.; Mascini, M.; Fiksdal, L. *Anal. Chim. Acta* **2001**, *427*, 149–154.
- (36) Mittelmann, A. S.; Ron, E. Z.; Rishpon, J. *Anal. Chem.* **2002**, *74*, 903–907.
- (37) Neufeld, T.; Schwartz-Mittelmann, A.; Biran, D.; Ron, E. Z.; Rishpon, J. *Anal. Chem.* **2003**, *75*, 580–585.
- (38) Cheng, Y.; Liu, Y.; Huang, J.; Xian, Y.; Zhang, W.; Zhang, Z.; Jin, L. *Talanta* **2008**, *75*, 167–171.
- (39) Wutor, V. C.; Togo, C. A.; Limson, J. L.; Pletschke, B. I. *Enzyme Microb. Technol.* **2007**, *40*, 1512–1517.
- (40) Hinks, J.; Han, E. J. Y.; Wang, V. B.; Seviour, T. W.; Marsili, E.; Loo, J. S. C.; Wuertz, S. *Microb. Biotechnol.* **2016**, *9*, 746–757.
- (41) Cheng, Y.; Liu, Y.; Huang, J.; Li, K.; Xian, Y.; Zhang, W.; Jin, L. *Electrochim. Acta* **2009**, *54*, 2588–2594.
- (42) Serra, B.; Morales, M. D.; Zhang, J.; Reviejo, A. J.; Hall, E. H.; Pingarron, J. M. *Anal. Chem.* **2005**, *77*, 8115–8121.
- (43) Togo, C. A.; Wutor, V. C.; Limson, J. L.; Pletschke, B. I. *Biotechnol. Lett.* **2007**, *29*, 531–537.
- (44) Christodouleas, D. C.; Nemiroski, A.; Kumar, A. A.; Whitesides, G. M. *Anal. Chem.* **2015**, *87*, 9170–9178.
- (45) Tryland, I.; Fiksdal, L. *Appl. Environ. Microbiol.* **1998**, *64*, 1018–1023.
- (46) Adkins, J. A.; Henry, C. S. *Anal. Chim. Acta* **2015**, *891*, 247–254.
- (47) Berg, K. E.; Adkins, J. A.; Boyle, S. E.; Henry, C. S. *Electroanalysis* **2016**, *28*, 679–684.
- (48) Ji, X.; Banks, C. E.; Crossley, A.; Compton, R. G. *ChemPhysChem* **2006**, *7*, 1337–1344.
- (49) Foster, C. W.; Metters, J. P.; Kampouris, D. K.; Banks, C. E. *Electroanalysis* **2014**, *26*, 262–274.
- (50) Palchetti, I.; Mascini, M. *Anal. Bioanal. Chem.* **2008**, *391*, 455–471.

- (51) Gui, A. L.; Liu, G.; Chockalingam, M.; Le Saux, G.; Luais, E.; Harper, J. B.; Gooding, J. J. *Electroanalysis* **2010**, *22*, 1824–1830.
- (52) Arvinte, A.; Mahosenaho, M.; Pinteala, M.; Sesay, A.-M.; Virtanen, V. *Microchim. Acta* **2011**, *174*, 337–343.
- (53) Yin, H.; Zhou, Y.; Ai, S.; Cui, L.; Zhu, L. *Electroanalysis* **2010**, *22*, 1136–1142.
- (54) Testa, A. C.; Reinmuth, W. H. *J. Am. Chem. Soc.* **1961**, *83*, 784–786.
- (55) Jokerst, J. C.; Adkins, J. A.; Bisha, B.; Mentele, M. M.; Goodridge, L. D.; Henry, C. S. *Anal. Chem.* **2012**, *84*, 2900–2907.
- (56) Mentele, M. M.; Cunningham, J.; Koehler, K.; Volckens, J.; Henry, C. S. *Anal. Chem.* **2012**, *84*, 4474–4480.
- (57) Santhiago, M.; Henry, C. S.; Kubota, L. T. *Electrochim. Acta* **2014**, *130*, 771–777.
- (58) Murdock, R. C.; Shen, L.; Griffin, D. K.; Kelley-Loughnane, N.; Papautsky, I.; Hagen, J. A. *Anal. Chem.* **2013**, *85*, 11634–11642.
- (59) Gerhart, J. C.; Pardee, A. B. *J. Biol. Chem.* **1962**, *237*, 891–896.
- (60) Reed, M. C.; Lieb, A.; Nijhout, H. F. *BioEssays* **2010**, *32*, 422–429.
- (61) Sabbah, R.; Gouali, M. *Aust. J. Chem.* **1994**, *47*, 1651–1660.
- (62) Lawrence, N. S.; Davis, J.; Compton, R. G. *Talanta* **2001**, *53*, 1089–1094.
- (63) Willford, J. D.; Bisha, B.; Bolenbaugh, K. E.; Goodridge, L. D. *Bacteriophage* **2011**, *1*, 101–110.
- (64) Hibbing, M. E.; Fuqua, C.; Parsek, M. R.; Peterson, S. B. *Nat. Rev. Microbiol.* **2010**, *8*, 15–25.
- (65) OECD, WHO. *Assessing Microbial Safety of Drinking Water Improving Approaches and Methods: Improving Approaches and Methods*; OECD Publishing: Paris, France, 2003.
- (66) Bisha, B.; Adkins, J. A.; Jokerst, J. C.; Chandler, J. C.; Pérez-Méndez, A.; Coleman, S. M.; Sbodio, A. O.; Suslow, T. V.; Danyluk, M. D.; Henry, C. S.; Goodridge, L. D. *J. Visualized Exp.* **2014**, DOI: [10.3791/51414](https://doi.org/10.3791/51414).
- (67) Bisha, B.; Perez-Mendez, A.; Danyluk, M. D.; Goodridge, L. D. *J. Food Prot.* **2011**, *74*, 1934–1937.
- (68) Hernández, L.; Hernández, P.; Vicente, J. *Fresenius' J. Anal. Chem.* **1993**, *345*, 712–715.